

Measurement of the shot noise in a single-electron transistor

S. Kafanov* and P. Delsing†

Microtechnology and Nanoscience, Chalmers University of Technology, S-41296 Göteborg, Sweden

(Received 17 March 2009; revised manuscript received 8 July 2009; published 19 October 2009)

We have systematically measured the shot noise in a single-electron transistor (SET) as a function of bias and gate voltages. By embedding a SET in a resonance circuit we have been able to measure its shot noise at the resonance frequency 464 MHz, where the $1/f$ noise is negligible. We can extract the Fano factor which varies between 0.5 and 1 depending on the amount of Coulomb blockade in the SET, in very good agreement with the theory.

DOI: [10.1103/PhysRevB.80.155320](https://doi.org/10.1103/PhysRevB.80.155320)

PACS number(s): 73.23.Hk, 07.50.Hp

I. INTRODUCTION

In both electronic and photonic devices the measured signal does not contain all the information about the state and dynamics of a system. In most cases there is additional information in the fluctuations of the signal.¹ For example, the shot noise in electronic circuits contains information about the charge of charge carriers. This was used by Saminadayar *et al.*² to demonstrate the fractional charge of the quasiparticles in a fractional quantum-Hall system. The shot noise can also reveal correlations of the charge carriers or photons. Bosons display bunching³ whereas fermions display antibunching due to the Pauli principle.^{4,5}

Electron tunneling in a tunnel junction or a point contact is described by a Poissonian process. If the transparency of the barrier T is small, the shot noise is proportional to T and the shot noise takes on the Schottky value $S=2e\langle I \rangle$, where $\langle I \rangle$ is the average current. To compare different situations the noise is often normalized to the Schottky value giving the so-called Fano factor $F=S/(2e\langle I \rangle)$.⁶ The Fano factor can be reduced, for example, in a quantum point contact where the transparency is large, then the shot noise is proportional to $T(1-T)$ for each of the participating channels.⁷⁻⁹ Another example is an array of identical series connected tunnel junctions, there the shot noise is inversely proportional to the numbers of junctions N , $S=2e\langle I \rangle/N$.¹⁰ The Fano factor can also be enhanced above unity which is the case when cotunneling dominates.

In a single-electron transistor (SET),^{11,12} where $N=2$, the tunneling is uncorrelated at high bias, and the shot noise is $S=e\langle I \rangle$, i.e., the Fano factor is 1/2. However, at low voltage the Coulomb blockade introduces correlations and the Fano factor increases. The correlation of tunnel events in a SET depends strongly on the biasing conditions and the amount of Coulomb blockade in the SET.

The shot noise in the SET is theoretically well understood both for dc operation¹³⁻¹⁶ and for the rf SET,^{17,18} however, so far a detailed comparison between experiment and theory has not been demonstrated. This is due to the fact that the shot noise in most cases is masked by other sources of noise. At low frequency, motion of background charge fluctuators give rise to $1/f$ noise,¹⁹ at higher frequencies the amplifier noise normally dominates over the shot noise. In a few cases the shot noise of double junction devices without a gate has been measured.²⁰⁻²² In other experiments on silicon and carbon

nanotube SETs the shot noise was studied with gate control. Sasaki *et al.*²³ studied a silicon SET and found a Fano factor lower than one half in the Coulomb blockade region in contradiction with theory. Onac *et al.*²⁴ studied a carbon nanotube SET and found superpoissonian shot noise with a Fano factor larger than unity, however there was no quantitative comparison to theory. Metallic SETs have been studied at high bias²⁵⁻²⁷ but the low-bias Coulomb blockade region where the correlations affect the Fano factor has so far not been studied. Metallic SETs in the superconducting state has recently been studied.²⁸

The single-electron transistor is formed by connecting two tunnel junctions in series and coupling a third electrode capacitively to the central island between the two junctions. The current through the SET is reduced by the additional charging energy, E_{ch} , which is needed to put a single electron onto the central island, this blocking of electron transport is referred to as the Coulomb blockade.²⁹ To get current flow through the SET one needs to apply a minimum bias voltage so that the potential energy of the electron overcomes the charging energy $eV > E_{ch}$. This defines the so-called threshold voltage $V_t = E_{ch}/e$. Since the charging energy depends on the gate charge, Q_g , the threshold voltage also becomes gate charge dependent and therefore the SET can be used as a very sensitive electrometer. If the current or conductance is plotted as a function of both bias voltage and gate charge a very characteristic pattern is formed with diamond-shaped areas along the gate charge axis, where the current or conductance is close to zero. Outside these diamonds there is larger current or conductance. Such a plot is referred to as a diamond plot or the stability diagram for the SET. The borders of the diamonds are referred to as the Coulomb threshold and defines the threshold voltage.

In this paper we present systematic measurements of the shot noise of a SET for different gate and bias voltages and we map out a similar diamond plot for the shot noise of the SET. We make a quantitative comparison with theory and show how the Fano factor varies between 0.5 and 1 depending on the correlations in the SET, in very good agreement with theory. We do this using a rf-SET setup³⁰ where a current is fed through the SET and the noise is coupled out to a cold amplifier via a resonance circuit [(Fig. 3(a)). In principle, the shot noise is frequency dependent,¹⁴ however since our measurements are done at a frequency much lower than the characteristic SET frequency $[1/(2\pi R_i C_i)] \sim 20$ GHz we are still in the low-frequency limit. Here R_i and C_i , i

$\in \{1, 2\}$ are the resistances and capacitances of the two junctions.

II. EXPERIMENT

The sample was fabricated from aluminum on an oxidized silicon substrate using electron-beam lithography and a standard double-angle evaporation technique. The sample was attached to the mixing chamber of a dilution refrigerator and cooled to a temperature of ~ 25 mK. All measurements were performed in the normal (nonsuperconducting) state at a magnetic field of 1.5 T. The SET was biased in the asymmetric mode with one lead grounded. The high-bias asymptotic resistance of the SET was $R \approx 72$ k Ω . The charging energy, $E_C/k_B = e^2/(2k_B C_\Sigma) \approx 2.5$ K was extracted from the measurements of the SET stability diagram, where C_Σ is the sum capacitance of the SET island. The asymmetry in the junction capacitances $\sim 30\%$ was deduced from the asymmetry of the SET stability diagram, see the inset of Fig. 3.

We have embedded the SET in an LC-resonance circuit, which transforms the high SET resistance to an impedance close to 50 Ω . The resonance circuit is connected via a superconducting coax to a low-noise cryogenic amplifier situated at 4.2 K. The coax is characterized by a wave impedance $Z_0 = 50$ Ω and a propagation constant β . We have assumed that the input and output impedances of the cryogenic amplifier are equal to Z_0 . The output signal from the cold amplifier is further amplified at room temperature and recorded with a spectrum analyzer.

The parameters of the matching circuit can be obtained from reflectometry measurements. A small rf signal at the resonance frequency f_{LC} is launched toward the SET and part of this signal is reflected from the circuit. The reflection coefficient, $\Gamma = (Z - Z_0)/(Z + Z_0)$, is the ratio between the voltages of the reflected and the incoming wave, and depends on the impedance mismatch between the resonance circuit impedance Z and Z_0 . The resonance frequency of the resonance circuit is defined by the LC parameters, $f_{LC} = 1/(2\pi\sqrt{LC})$ and was measured to 464 MHz [see Fig. 1(b)].

In our measurements the SET differential resistance R is always much larger than the impedance of the transmission line, $R \gg Z_0$ and we perform the measurements at the resonance frequency, $f = f_{LC}$. In this case Γ is real and given by $\Gamma = (Z_{LC}/R - Z_0/Z_{LC})/(Z_0/Z_{LC} + Z_{LC}/R)$. $Z_{LC} = \sqrt{L/C}$ is the characteristic impedance of the LC circuit (not including R).

The shot noise from the SET can be described as a current-noise source i_s in parallel with the SET, as shown in Fig. 1(a). The power spectral density of the shot noise is given by the Fano factor F and the current through the SET, $\langle i_s^2 \rangle = 2e\langle I \rangle F$. Considering the electrical scheme in Fig. 1(a), and taking into account that $R \gg Z_0$, we can calculate the power spectral density at the amplifier output, resulting from the shot noise of the SET, as a function of the resonance circuit parameters

$$S_{shot} = \frac{g^2 Z_0 \langle i_s^2 \rangle}{[1 - (f/f_{LC})^2]^2 + (f/f_{LC})^2 (1/Q)^2}, \quad (1)$$

where g is the amplifier voltage gain and $Q = (Z_{LC}/R + Z_0/Z_{LC})^{-1}$ is the total quality factor of the resonance circuit.

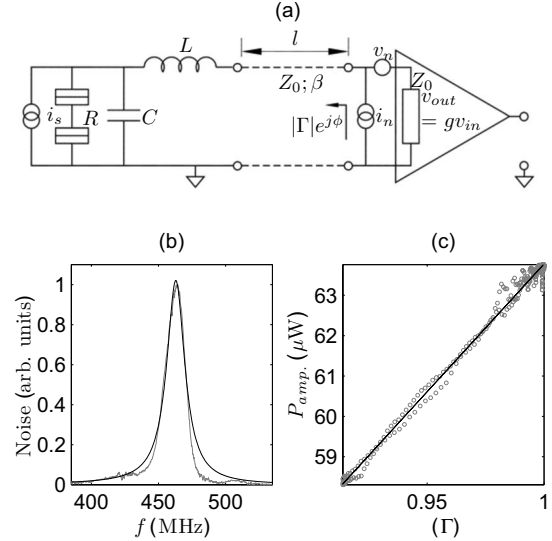


FIG. 1. (a) Simplified circuit scheme for the shot noise measurements with a rf SET. The resonance circuit is connected to the microwave amplifier via a transmission line with a characteristic impedance Z_0 and propagation constant β . The transmission line produces a phase delay $-\beta l$. (b) Resonance curve for the resonance circuit. The light gray curve is the measured noise power as a function of frequency. The black curve is a fit to Eq. (1). (c) The measured amplifier noise as a function of the magnitude of the reflection coefficient (circles). The continuous line is a fit to Eq. (3).

The detected shot noise has a Lorentzian line shape as can be seen in Fig. 1(b).

III. MEASUREMENT RESULTS

To be able to extract the Fano factor we have done three different measurements. For each bias voltage, V , we have measured Γ and the output noise from the amplifier, as we swept the gate charge, Q_g . This was done for 80 different bias voltages. To calibrate the amplifier noise we have in addition measured the amplifier output noise at zero bias as a function of gate charge.

The noise measurements were done at f_{LC} with a bandwidth, $\Delta f = 15$ kHz, significantly narrower than the resonance circuit bandwidth. In this case, the power spectral density of the shot noise can be expressed as a function of the magnitude of the reflection coefficient

$$S_{shot} = (g^2/8)R(1 - |\Gamma|^2)\langle i_s^2 \rangle = (g^2/4)(1 - |\Gamma|^2)eFV. \quad (2)$$

There is a clear advantage to express both the shot noise and the amplifier noise in terms of $|\Gamma|$ rather than the SET resistance since parasitics of the tank circuit such as the shunt capacitance of the inductance is automatically included in $|\Gamma|$.

The SET-generated noise for maximum Coulomb blockade, $Q_g \approx 0$, and the SET open state, $Q_g \approx 0.5e$, is shown in Fig. 2. The inset shows the full set of data for all bias points. Here, the amplifier noise has been subtracted as will be explained later in the text. As can be seen there is no noise signal inside Coulomb blockade, when there is no current

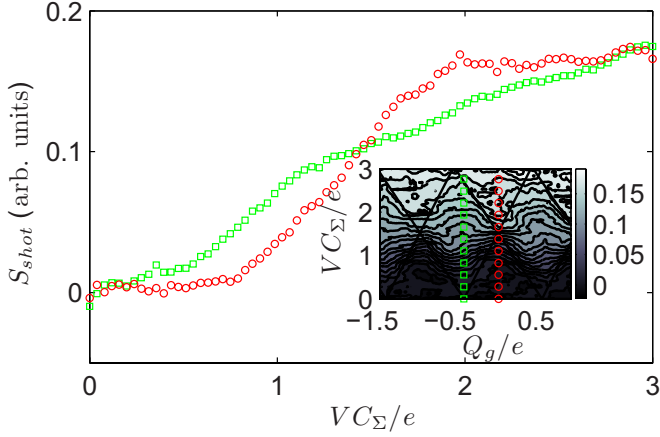


FIG. 2. (Color online) The shot noise generated by the single-electron transistor as a function of bias voltage. The square marks shows the noise at maximum Coulomb blockade. The circle marks shows the noise when the SET is in its open state. The amplifier noise has been subtracted as described in the text. The noise is measured at the resonance frequency in a bandwidth of a 15 KHz. The inset shows a color map of the shot noise as a function of both bias voltage and gate charge.

through the SET. For high bias voltages (data not shown), where the SET resistance reaches its asymptotic value, and $|\Gamma|$ remains constant, the noise increases linearly with bias.

As can be seen from Eq. (2), we also need to measure $|\Gamma|$ at the same bias conditions in order to extract the Fano factor. Here we have normalized $|\Gamma|$ to unity in the Coulomb blockade region. In Fig. 3 we show the experimentally measured $|\Gamma|$ versus bias for maximum Coulomb blockade and for the SET open state. The inset shows the full bias-gate dependence. $|\Gamma|$ decreases monotonically from unity at low bias to the asymptotic value $|\Gamma|=0.7$ at high bias. Thus, we conclude that the SET is operated in the overcoupled regime, where the impedance of the resonance circuit $Z=Z_{LC}^2/R$ is always smaller than Z_0 .

A. Calibrating the amplifier noise

The noise at the output of the amplifier also has a contribution from the amplifier itself, which should be accounted for. Generally the amplifier noise depends on the impedance of the resonance circuit. We describe the noise sources of the amplifier and refer them to the amplifier input.³¹ In general two noise sources are required: a series voltage-noise source v_n , and a shunt current-noise source i_n , as shown in the Fig. 1(a). The current-noise source is due to the input current of the first high electron mobility transistor (HEMT). The voltage-noise source represents the internal amplifier noise referred to the input of the amplifier. The noise power at the output of the amplifier will clearly depend on the impedance attached to the input of the amplifier. We can express also the amplifier noise as a function of $|\Gamma|$,

$$S_{amp} = \frac{g^2}{8} [(1 + |\Gamma|^2) (\langle i_n^2 \rangle Z_0 + \langle v_n^2 \rangle / Z_0) + 2|\Gamma| \cos(\phi - 2\beta l) \times (\langle i_n^2 \rangle Z_0 - \langle v_n^2 \rangle / Z_0)], \quad (3)$$

where ϕ is the phase of the voltage reflection from the reso-

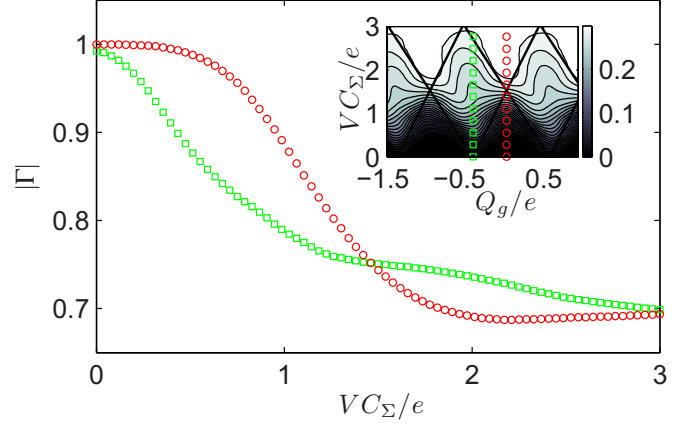


FIG. 3. (Color online) The magnitude of the reflection coefficient as a function of the SET bias voltage. The circle marks corresponds to the maximum of the Coulomb blockade. The square marks corresponds to the SET open state. The inset shows color map of $|\Gamma|$ as a function of both bias voltage and gate charge.

nance circuit and $-2\beta l$ is the phase delay in the coaxial cable. Amplifiers are normally optimized so that the voltage noise and the current-noise contributions are equally large for a source impedance of Z_0 and therefore the second term in Eq. (3) is very small and can be neglected. However, it is worth noting that if the two noise sources are not balanced, the influence of the amplifier noise can be substantially decreased by choosing the proper length of the transmission line between the amplifier and the resonance circuit.

To calibrate the amplifier noise, the SET was biased at zero voltage, and the output amplifier noise was measured as a function of the SET gate charge, Γ was measured for the same gate charges. The conductance of an SET at zero bias varies between zero and $1/[2(R_1+R_2)]$. For a given resonance circuit this sets a lower limit for the reflection coefficient at zero bias, in our case this limit is 0.91. For higher bias the conductance can be higher, but then shot noise is also added, which means that we cannot use a finite bias to measure the amplifier part of the noise. Thus we only have calibration data for Γ between 0.91 and 1.0 and we need to extrapolate the data to be able to subtract the amplifier noise in the whole range $0.7 < |\Gamma| < 1$. We do this by plotting the amplifier noise as a function of $|\Gamma|$ in the range $(0.91 < |\Gamma| < 1)$ and fit it to Eq. (3) as shown in Fig. 1(c). The amplifier noise is well fitted by Eq. (3) neglecting the second term. The amplifier noise can then be subtracted from the measured noise using Eq. (3) so that we obtain the bare shot noise signal. Finally we combine Eqs. (2) and (3) to extract the Fano factor over the hole range of bias and gate voltage, the result is plotted in Fig. 4(a).

$$F(V, Q_g) = \frac{S_{meas}(V, Q_g) - S_{amp}(|\Gamma|)}{(g^2/4)(1 - |\Gamma|^2)eV}. \quad (4)$$

There is some uncertainty in the amplifier voltage gain g and we have used the asymptotic value of the Fano factor at high bias to set the gain in Fig. 4(a). The Fano factor asymptotic value is weakly dependent on the tunnel junctions resistances.¹⁴ Assuming that the resistance asymmetry

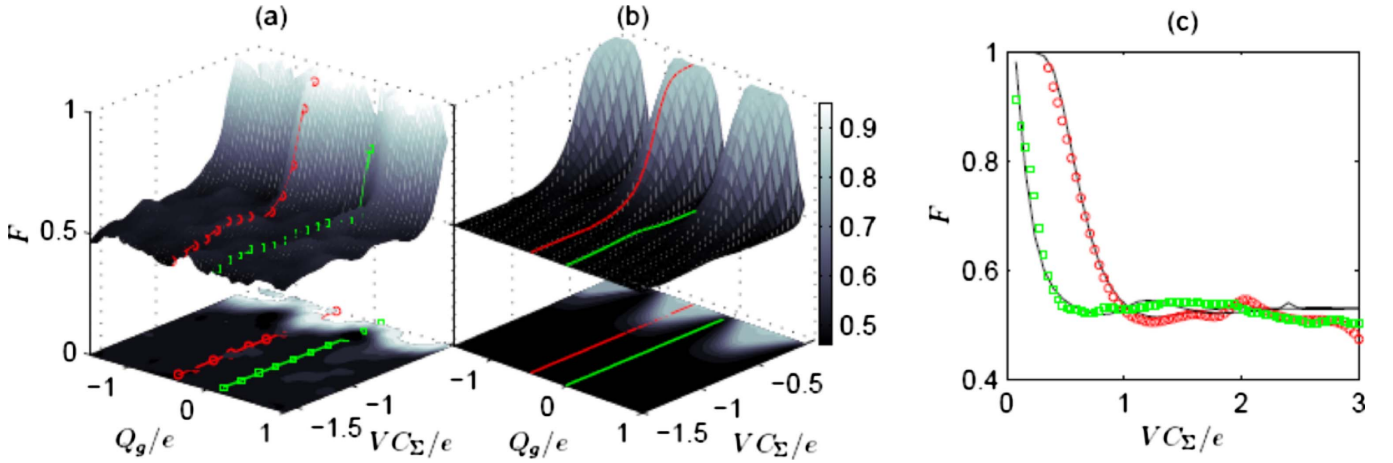


FIG. 4. (Color online) (a) The measured Fano factor for the SET as a function of bias voltage V and gate charge Q_g , the marked lines are the line cuts shown in panel (c) for fixed Q_g . (b) The calculated Fano factor as a function of bias voltage V and gate charge Q_g . The calculation is done using the orthodox theory (Refs. 14 and 29) for single-electron tunneling, neglecting cotunneling. We have assumed that transistor is overheated from the cryostat base temperature $T \approx 0.1E_c = 250$ mK. (c) Measured Fano factor as a function of bias voltage for open state (square markers) and maximum Coulomb blockade (circle markers). The black lines are the corresponding calculations using the orthodox theory (Ref. 14).

is the same as the capacitances asymmetry in the tunnel junctions (30%), the asymptotic Fano factor value should be: $F = (R_1^2 + R_2^2) / (R_1 + R_2)^2 \approx 0.51$.

Figure 4(a) represents the main result of our work, it shows a complete map of the Fano factor as a function of both bias voltage and gate charge. F is close to 0.5 at high bias and increases to unity as the bias is lowered toward the Coulomb threshold. Close to the threshold F varies between 0.5 and 1 as a function of gate charge. In the Coulomb blockade region both the shot noise and the current goes to zero and the Fano factor loses its meaning.

B. Comparison to theory

The theory of shot noise in the SETs was developed in the early 1990s.^{13–16} Current transport through an individual ideal tunnel barrier is a totally uncorrelated flow of charge carriers and the noise is described by Poissonian statistics of individual tunnel events. The power spectral density for this process is given by the Schottky formula and is a frequency-independent function up to frequencies corresponding to the transit time of a charge carrier through the tunnel barrier. Electron-electron interactions, resulting from the Pauli exclusion principle, or resulting from electrostatic Coulomb interactions, can result in correlated electron motion and usually suppresses the shot noise and lead to a lower Fano factor. In the case of two tunnel junctions connected in series such as the SET, the transport becomes correlated due to electrostatic interaction and the Fano factor should then in general be one.

For limiting cases the shot noise can be expressed analytically. In the limit of low bias and nonzero temperature ($E_c > eV > k_B T$) the current through the SET is essentially determined by one of the two junctions. Thus, the shot noise in the Coulomb blockade region assumes the Poissonian value $S = 2eI$, i.e., and the Fano factor is equal to unity. At higher bias voltage, above the Coulomb blockade threshold

($eV > E_c > k_B T$), the current becomes uncorrelated, In this limit, both junctions will be important and therefore the Poissonian noise is suppressed and the Fano factor will given by $(R_1^2 + R_2^2) / (R_1 + R_2)^2$.

The shot noise can be explained in the standard orthodox model of single-electron tunneling,²⁹ which neglects higher-order tunnel events (cotunneling) and assumes a low impedance environment for the SET. Korotkov¹⁴ has calculated the shot noise which depends on the tunnel rates in the different junction and the conditional probability $\sigma_{n,t,m,t'}$ for having n electrons in the SET island at the time t under the condition that there were m electrons at the earlier time t' . The probabilities can be extracted from the steady-state solution of a rate equation including the rates mentioned above. The low-frequency shot noise in the SET is given by Eq. 35.¹⁴ We have numerically calculated the shot noise for our sample parameters using this equation. In these calculations we have used the capacitances and resistances extracted above, we have included five charge states on the SET island and neglected cotunneling. The only free parameter is the temperature of the SET island. In our calculations we have taken into account that the SET is substantially overheated from the cryostat base temperature. Using a SET temperature of $T \approx 0.1E_c/k_B = 250$ mK gives a very good agreement between experiment and theory. This is a number which agrees well with other measurements of the overheating in SETs.³² In Fig. 4(b) we show the calculated Fano factor as function of bias voltages and gate charge using the orthodox theory of single-electron tunneling as described above.

Especially interesting cases are when the SET is fully open, $Q_g = 0.5e$ and when the Coulomb blockade is maximum, $Q_g = 0$. These two cases are show in Fig. 4(c), the circle and square marks are experimental data for $Q_g = 0.5e$ and $Q_g = 0$, respectively. The continuous lines are the calculations using the orthodox theory.

IV. CONCLUSION

The measurements shown here demonstrate the correlations of tunneling in the single-electron transistor, which are well understood. At low voltages, the tunneling is limited by the rate in one of the junctions and the tunneling becomes correlated giving a Fano factor close to unity since the SET then behaves more like a single junction. At high bias the tunneling in the two junctions is sequential and uncorrelated, which results in the reduced shot noise $2e\langle I \rangle/N$. Using the method described here it should be possible to study also more complicated correlations in the SET including cotunneling and also combined Cooper-pair quasiparticle processes which occur when the SET is in the superconducting state.

In conclusion we have introduced a method for shot noise measurements of mesoscopic systems embedded in a reso-

nance circuit. The measurements are done at a finite frequency where the $1/f$ noise can be neglected. We have been able to measure the shot noise generated by a single-electron transistor as a function of both bias and gate voltages. From the data we can extract the Fano factor which varies between 0.5 and 1 depending on the amount of correlation of the tunneling in the two junctions. Our experimental results agree very well with the orthodox theory for single-electron tunneling.

ACKNOWLEDGMENTS

We would like to acknowledge helpful discussions with J. Clarke, T. Duty, G. Johansson, and C. Wilson. The samples were made at the MC2 clean room at Chalmers. This work was supported by the Swedish SSF and VR, and by the Wallenberg foundation.

*Present address: Low Temperature Laboratory, Helsinki University of Technology, P.O. Box 3500, 02015 TKK, Finland. sergey.kafanov@ltd.tkk.fi

†per.delsing@chalmers.se

¹R. Landauer, *Nature (London)* **392**, 658 (1998).

²L. Saminadayar, D. C. Glatli, Y. Jin, and B. Etienne, *Phys. Rev. Lett.* **79**, 2526 (1997).

³R. Hanbury-Brown and R. Q. Twiss, *Nature (London)* **178**, 1447 (1956).

⁴M. Henny, S. Oberholzer, C. Strunk, T. Heinzel, K. Ensslin, M. Holland, and C. Schönberger, *Science* **284**, 296 (1999).

⁵W. D. Oliver, J. Kim, R. C. Liu, and Y. Yamamoto, *Science* **284**, 299 (1999).

⁶U. Fano, *Phys. Rev.* **72**, 26 (1947).

⁷G. Lesovik, *JETP Lett.* **49**, 592 (1989).

⁸A. Kumar, L. Saminadayar, D. C. Glatli, Y. Jin, and B. Etienne, *Phys. Rev. Lett.* **76**, 2778 (1996).

⁹M. Reznikov, M. Heiblum, H. Shtrikman, and D. Mahalu, *Phys. Rev. Lett.* **75**, 3340 (1995).

¹⁰A. N. Korotkov, *Phys. Rev. B* **50**, 17674 (1994).

¹¹K. Likharev, *IEEE Trans. Magn.* **23**, 1142 (1987).

¹²T. A. Fulton and G. J. Dolan, *Phys. Rev. Lett.* **59**, 109 (1987).

¹³A. Korotkov, D. Averin, K. Likharev, and S. Vasenko, in *Single-Electron Tunneling and Mesoscopic Devices*, edited by H. Koch and H. Lübbig (Springer, Berlin, 1992), p. 45.

¹⁴A. N. Korotkov, *Phys. Rev. B* **49**, 10381 (1994).

¹⁵S. Hershfield, J. H. Davies, P. Hylgaard, C. J. Stanton, and J. W. Wilkins, *Phys. Rev. B* **47**, 1967 (1993).

¹⁶U. Hanke, Y. M. Galperin, and K. A. Chao, *Phys. Rev. B* **50**, 1595 (1994).

¹⁷A. N. Korotkov and M. A. Paalanen, *Appl. Phys. Lett.* **74**, 4052 (1999).

¹⁸J. H. Oh, D. Ahn, and S. W. Hwang, *Phys. Rev. B* **72**, 165348 (2005).

¹⁹G. Zimmerli, T. Eiles, R. Kautz, and J. Martinis, *Appl. Phys. Lett.* **61**, 237 (1992).

²⁰H. Birk, M. J. M. de Jong, and C. Schönberger, *Phys. Rev. Lett.* **75**, 1610 (1995).

²¹A. Nauen, I. Hapke-Wurst, F. Hohls, U. Zeitler, R. J. Haug, and K. Pierz, *Phys. Rev. B* **66**, 161303(R) (2002).

²²A. Nauen, F. Hohls, N. Maire, K. Pierz, and R. J. Haug, *Phys. Rev. B* **70**, 033305 (2004).

²³S. Sasaki, K. Tsubaki, S. Tarucha, A. Fujiwara, and Y. Takahashi, *Solid-State Electron.* **42**, 1429 (1998).

²⁴E. Onac, F. Balestro, B. Trauzettel, C. F. J. Lodewijk, and L. P. Kouwenhoven, *Phys. Rev. Lett.* **96**, 026803 (2006).

²⁵A. Aassime, G. Johansson, G. Wendin, R. J. Schoelkopf, and P. Delsing, *Phys. Rev. Lett.* **86**, 3376 (2001).

²⁶A. Aassime, D. Gunnarsson, K. Bladh, P. Delsing, and R. Schoelkopf, *Appl. Phys. Lett.* **79**, 4031 (2001).

²⁷L. Roschier, P. Hakonen, K. Bladh, P. Delsing, K. W. Lehnert, L. Spietz, and R. J. Schoelkopf, *J. Appl. Phys.* **95**, 1274 (2004).

²⁸W. Xue, Z. Ji, F. Pan, J. Stettenheim, and A. Rimberg, *Nat. Phys.* **5**, 660 (2009).

²⁹D. Averin and K. Likharev, in *Mesoscopic Phenomena in Solids*, edited by B. Altshuler, P. Lee, and R. Webb (North-Holland, Amsterdam, 1991), p. 173.

³⁰R. J. Schoelkopf, P. Wahlgren, A. Kozhevnikov, P. Delsing, and D. E. Prober, *Science* **280**, 1238 (1998).

³¹B. Schiek, I. Rolfes, and H.-J. Siweris, *Noise in High-Frequency Circuits and Oscillators* (Wiley, New York, 2006).

³²S. M. Verbrugh, M. L. Benhamadi, E. H. Visscher, and J. E. Mooij, *J. Appl. Phys.* **78**, 2830 (1995).